J Ind Microbiol Biotechnol (2014) 41:1181–1190
DOI 10.1007/s10295-014-1454-z

BIOCATALYSIS

SIMB
Society for Industrial Microbiology and Biotechnology

Enhancing the activity of *Bacillus circulans* xylanase by modulating the flexibility of the hinge region

Fukura Kazuyo · So Yeon Hong · Young Joo Yeon · Jeong Chan Joo · Young Je Yoo

Received: 21 December 2013 / Accepted: 28 April 2014 / Published online: 22 May 2014

Abstract Enzymes undergo multiple conformational changes in solution, and these dynamics are considered to play a critical role in enzyme activity. Hinge-bending motions, resulting from reciprocal movements of dynamical quasi-rigid bodies, are thought to be related to turnover rate and are affected by the physical properties of the hinge regions. In this study, hinge identification and flexibility modification of the regions by mutagenesis were conducted to explore the relationship between hinge flexibility and catalytic activity. *Bacillus circulans* xylanase was selected for the identification and mutation of the hinge regions. As a result, turnover rate (V_{max}) was improved approximately twofold in mutants that have more rigid hinge structure, despite the decrease in K_m and V_{max}/K_m. This result indicates that the rigidly mutated hinge has positive effects on *B. circulans* xylanase activity.

Keywords Xylanase · Activity · Dynamics · Flexibility · Hinge

F. Kazuyo · S. Y. Hong · Y. J. Yoo (✉)
Graduate Program of Bioengineering, Seoul National University, Seoul 151-742, Republic of Korea
e-mail: yjyoo@snu.ac.kr

Y. J. Yeon · J. C. Joo · Y. J. Yoo
School of Chemical and Biological Engineering, Seoul National University, Seoul 151-742, Republic of Korea

J. C. Joo
Department of Chemical Engineering and Applied Chemistry, University of Toronto, Toronto, ON M5S 3E5, Canada

Y. J. Yoo
Bio-MAX Institute, Seoul National University, Seoul 151-742, Republic of Korea

Introduction

Enzymes have major advantages in the synthetic industry in terms of high selectivity, molecule conversion at ambient conditions, low energy consumption and low byproduct formation. Due to these features, biocatalysis is regarded as an environmentally friendly method for the synthesis of chemicals and can lead to overall process cost reduction [22]. Successful application of enzymes in the synthetic industry requires increased product titer and enhanced catalytic efficiency. Methods used to enhance biocatalytic efficiency include enzyme screening, inhibitor removal, activator addition and protein engineering. Among these methods, in this study, protein engineering was applied to enhance enzyme activity. Two broad approaches have been taken in enzyme engineering, namely, directed evolution and rational design. Whereas the former uses a random mutational strategy, the latter can obtain the required enzyme improvements on a logical basis using structure and sequence information. Rational design is therefore preferred for enzyme design if the required information is available. However, there have been few research reports on applying rational design for enhancing enzyme activity and especially few reports describing a general strategy.

Enzymes are dynamic and flexible molecules that exhibit oscillating motions known to be related to the catalytic function [5, 27]. Dynamic substructures have been noted due to the subunit motions observed in the functional cycles of many enzymes [21]. The flexibility of each part of the enzyme contributes to maintaining protein structure and functional activity. Due to this function–dynamics relationship, there is growing interest in the investigation of domain (or protein subunit) motions [21]. Such quasi-rigid bodies can move through reciprocal interactions, while their own folds remain essentially unaffected. There occurs

a fixed boundary region between two motional subunits of a protein; in enzymes, this region is defined as a hinge. The hinge region is observed in many enzymes exhibiting hinge-bending motions that alter the relative distance between large rigidly moving regions.

In this study, *Bacillus circulans* xylanase (Bcx) was used as a model enzyme. This enzyme belongs to a group of endo-1,4-β-xylanases (E.C. 3.2.1.8), which is an important enzyme with a wide range of industrial applications in pulp bleaching, beverage, food, detergent, antimicrobial agents, and bioconversion of lignocelluloses [23]. An analysis of the enzyme structure was performed focusing on the pivot residues, which act as mechanical hinge and are located in the linker region between moving quasi-rigid bodies. The hinge region is considered to have a role in promoting or sustaining the conformational change required for catalysis [20]. In the case of hydrolase, which is functionally similar to xylanase, the catalytic site is located near the inter-domain region between the two quasi-rigid bodies [17]. The inter-domain region is important for precisely maintaining the geometry of the active site while allowing for a functionally oriented modulation of the adjacent regions resulting from the reciprocal action of the two subunits.

The objective of this work is the identification of the relationship between hinge flexibility and enzyme activity. The flexibility of the hinge region was studied using site-directed mutagenesis of a few residues on or near the hinge region to elucidate the relationship between rigidity level and catalytic activity. The selected residues were substituted with several amino acids with different flexibilities with regard to B-factor profiles, and the changes in intra-protein interactions were investigated.

Materials and methods

Computational analysis

Hinge identification

The protein decomposer PiSQRD was used to subdivide Bcx into several approximately rigid units. The web-based program groups amino acids into pre-assigned numbers by the pair-wise distances between sets of two amino acids that remain unaltered in the course of protein equilibrium fluctuations [17]. The substrate free and bound forms of Bcx, PDB ID: 1XNB and 1BVV were subdivided into groups numbered from 2 to 7. After application in every pre-assigned grouping number, the boundary residues coinciding over five subdivisions were selected in both structures. Finally, the overlapping residues in the two groups (apo and holo) were chosen as the hinge region of Bcx.

In silico mutation

SCWRL4 was used to carry out in silico mutations used to simulate the results of mutating target residues. The program predicts side chain conformations of substituted amino acids [10].

Flexibility analysis

The flexibility indices of amino acids were used to predict the flexibility of any given amino acid. The flexibility index correlates with the tendency of the side chain to be buried or exposed, which provides information on the likelihood that a certain amino acid will be rigid or flexible in the globular amino acid chain [18].

Intra-protein interactions

Protein interactions calculator (PIC) was used to calculate enzyme interactions. This web server identifies various types of interactions, such as disulphide bonds, hydrophobic interactions, ionic interactions, hydrogen bonds, aromatic–aromatic interactions, aromatic–sulphur interactions and cation–pi interactions, within a protein [25]. The structures of Bcx and the mutants generated by in silico mutation were used to recognize the internal interactions.

Residual flexibility

Floppy inclusions and rigid substrate topography (FIRST) and framework rigidity optimized dynamics algorithm (FRODAN) on the Flexweb server were used to calculate the residual flexibility of Bcx. FIRST is software that identifies rigidity and flexibility in network graphs, and FRODAN predicts dynamics according to the static results of the FIRST analysis [26]. The substrate free and bound structures 1XNB and 1BVV were calculated using momentum as a motion type until 5,000 conformers were generated.

Biomolecular and chemical materials

The *bcx* synthetic gene (GeneBank Accession Number: P09850) was a generous gift from Department of Biochemistry and Molecular Biology, University of British Columbia. The properties and detailed preparation procedure for this gene are described in the previous studies [15, 24]. Restriction enzymes (*Nhe*I, *Xho*I and *Dpn*I) and P*fu* DNA polymerase were obtained from NEB (Ipswich, MA, USA) and Bioneer (Daejeon, Korea), respectively. Competent *E. coli* strains Top10 and BL21 (DE3) were obtained from Invitrogen (Carlsbad, CA, USA) and Novagen (Madison, WI, USA), respectively. Ni-NTA agarose for his-tag purification was obtained from Qiagen (Valencia, CA, USA).

Table 1 Primers of Bcx variants

Enzymes	Template	Primers
Wild-type Bcx	Synthetic gene	Forward: 5′GGGCCCGGGGCTAGCATGACTGGT3′ Reverse: 5′GGGCCCGGGCTCGAGTGCGGCCGCAGG3′
V131S	p23bBcx	Forward: 5′CAGTATTGGAGTAGTAGACAATCTAAGCGGCCGACTG3′ Reverse: 5′CGCTTAGATTGTCTACTACTCCAATACTGAGTAAAGG3′
R132 M	p23bBcx	Forward: 5′CAGTATTGGAGTGTTATGCAATCTAAGCGGCCGACTG3′ Reverse: 5′CGCTTAGATTGCATAACACTCCAATACTGAGTAAAGG3′
R132L	p23bBcx	Forward: 5′CAGTATTGGAGTGTTTTACAATCTAAGCGGCCGACTG3′ Reverse: 5′CGCTTAGATTGTAAAACACTCCAATACTGAGTAAAGG3′
N141G	p23bBcx	Forward: 5′GTTCGGGCGCCACCATTACGTTCACCAATCAC3′ Reverse: 5′GTGGCGCCCGAACCAGTCGGCCGCTTAGATTG3′
N141T	p23bBcx	Forward: 5′GACTGGTTCGACCGCCACCATTACGTTCACCAATC3′ Reverse: 5′GTAATGGTGGCGGTCGAACCAGTCGGCCGCTTAG3′
N141V	p23bBcx	Forward: 5′GACTGGTTCGGTCGCCACCATTACGTTCACCAATC3′ Reverse: 5′GTAATGGTGGCGACCGAACCAGTCGGCCGCTTAG3′
A142I	p23bBcx	Forward: 5′GACTGGTTCGAACATCACCATTACGTTCACCAATC3′ Reverse: 5′GTAATGGTGATGTTCGAACCAGTCGGCCGCTTAG3′

BSA protein and dye reagent for the protein assay were obtained from Bio-RAD (Hercules, CA, USA). Polymeric xylan substrate beechwood xylan and xylose for the product standard curve were obtained from Sigma (St. Louis, USA). SYPRO Orange dye was purchased from Invitrogen (Carlsbad, CA, USA).

Site-directed mutagenesis

The xylanase gene was PCR-amplified from the synthetic *bcx* gene. The primers used in this study are listed in Table 1. The amplified fragments were digested by *Nhe*I and *Xho*I and then cloned into the multi-cloning site of the pET-23b(+) vector (Novagen, USA) restricted by the same restriction enzymes to produce the recombinant plasmid p23bBcx. Site-specific mutants were generated using the efficient primer design method described by Zheng et al. [28], which is based on the Quik-change site-directed mutagenesis protocol [3]. The PCR mixture (total volume of 50 µl) consisted of the recombinant plasmid p23bBcx (1 µl) as template DNA, complementary designed primers (1 µl for both forward and reverse), P*fu* DNA polymerase (1 µl) and P*fu* buffer (47 µl). The polymerase chain reaction was performed as described by Zheng et al. [28]. The PCR products were purified using a PCR purification kit and incubated in a restriction reaction with *Dpn*I at 37 °C for 2 h to remove the methylated template. The restricted genes were transformed to *E. coli* Top10 using heat shock (42 °C for 90 s). The successfully transformed cells were selected by incubating on LB agar plates supplemented with 50 µg/ml of ampicillin and were then cultured in 3 ml LB media supplemented with 50 µg/ml of ampicillin. The mutant plasmids were isolated for sequencing, and the mutations were verified by Cosmogenetech (Daejeon, Korea).

Expression and purification of enzyme

The constructed plasmid was transformed into *E. coli* BL21 (DE3) by heat shock (42 °C for 90 s). The transformants carrying genes of wild-type and mutant xylanases were cultivated in 200 ml LB media supplemented with 50 µg/ml of ampicillin at 37 °C. IPTG (1 mM) was added at 0.4–0.6 absorbance at 600 nm to induce enzyme expression, and cultivation was continued at 20 °C for 24 h to prevent protein aggregates [19]. The cells were harvested by centrifugation and resuspended in lysis buffer (50 mM sodium phosphate, 300 mM NaCl, and 10 mM imidazole). The cells were lysed by sonication on ice (3 s pulse, 5 s pause, 100 W for 20 min), and the supernatant was separated from the cell debris by centrifugation [11,591×*g* (8,000 rpm), 20 min].

The recombinant xylanases were purified on a Ni-NTA agarose column. 20 ml of the supernatant was mixed with 1 ml of the Ni-NTA resin at 4 °C for 1 h. The resin was washed with 50 ml of wash buffer (50 mM sodium phosphate, 300 mM NaCl, and 40 mM imidazole) and then, eluted with elution buffer (50 mM sodium phosphate, 300 mM NaCl, and 250 mM imidazole) in purification column. Enzyme purity was assessed by analysis on 12 % SDS-PAGE. Determination of enzyme concentration was carried out using a modified Bradford assay [2] according to the manufacturer's instructions.

Enzyme activity and kinetic parameters

Enzyme activity was assayed using a modified dinitrosalicylic (DNS) acid method described by Bailey et al. [1] with beechwood xylan as a substrate. The reaction mixture

containing 100 ng/ml enzyme (40 µl) and 1 % (w/v) xylan solution (360 µl) was incubated at 40 °C for 5 min, after which DNS solution (600 µl) was added to stop the reaction. The mixture was heated to boiling for 2 min and then cooled for 2 min. In this method, the activity was assessed by measuring the release of oligosaccharides and reducing sugars that react with DNS acid. After the reaction, the absorbance of the color-developed mixture was measured at 540 nm. One unit of xylanase activity was interpreted as the amount of enzyme required to generate 1 µmol of the reducing sugars in 1 min at 40 °C using xylose as a standard product. The standard curve of xylose in the range of 0.40–10 mM was prepared for every series of assays to minimize variation due to, e.g., different batches of substrate and DNS, boiling conditions [1].

A kinetic assay was carried out at 40 °C with substrate concentrations in the range of 0.05–1.2 % (w/v), and the kinetic parameters (K_m and V_{max}) were calculated using the Lineweaver–Burk equation. All kinetic parameters were the means of triplicate measurements.

Thermostability

Thermodynamic stability of the wild-type and mutant xylanases was measured using differential scanning fluorimetry (DSF) to determine the temperatures at the midpoint of melting transition (T_m). A real-time quantitative PCR thermal cycler (LightCycler 480, Roche, USA) was used and purified proteins (0.2–0.5 mg/ml) mixed with a 20× solution of SYPRO Orange dye in 96-well qPCR microplates were heated from 20 to 95 °C at 1 °C/min scan rate. The T_m values are the mean values of triplicate measurements.

Results and discussion

Hinge region identification

Hinge regions were identified using the computational tool PiSQRD. As a result, four hinge regions were identified (Table 2). Of the four regions, two (129–135, 159–160) were identified to be located at or near the putative hinge of the *Trichoderma reesei* xylanase [14] when superimposing both structures. The other two regions were located in the hinge axes formed when comparing substrate-bound and free conformations. This result was further analyzed by the fluctuation calculating webserver FIRST (FRODAN) (Fig. 1).

In many cases, more than one conformation was crystallized from a protein, and dynamic domains were found by observing the structure in different states. These domains may be defined as residual groups moving in a concerted manner [7], with hinge regions between the domains.

Table 2 Identified hinge residues by PiSQRD

Position in Bcx	Identified by PiSQRD
Finger (back of hand)	50–51
Between thumb and finger (near thumb)	129–135
Between thumb and finger (near finger)	141–145
Between helix and finger	159–160

PiSQRD was run to decompose the model enzyme Bcx in terms of equilibrium fluctuations, and apo and holo forms were decomposed into pre-assigned numbers of quasi-rigid bodies (between 2 and 7). Within the intervening residues between the quasi-rigid bodies in each clustering number, the most commonly detected residues over four clustering modes in the two structures (apo and holo) were identified as the hinge regions (Table 2). These regions are regarded as hinge regions within the conformational selection model [13], which assumes dynamically changing populations of molecules.

As previously described, a hinge region is defined as a fixed boundary region between moving subunits; in other words, the region contains residues that fluctuate less than neighboring moving residues. FIRST 6.2 was run to estimate the fluctuation of each residue with default parameters other than the energy cutoff, which was set to −2.4 kcal/mol; the results are shown in Fig. 1 and Table 3. In Fig. 1, the continuous line represents the mean value of the residual fluctuation of the entire residue. This result shows that most of the RMSD values of the identified hinge regions are relatively lower than those of the entire residues. This indicates that the hinges were detected in neighboring regions to high-motion subunits, which is well in accord with the hinge region definition.

Selection of the target sites and mutation

The selection of the target hinge sites was carried out by a case-specific investigation of the model enzyme Bcx. Of the four hinge regions (Table 2; Fig. 2) identified by computational tools, Arg49 in the hinge region of 49–51 (R49N, R49E, R49Q) and His156 near the region of 159–160 (H156V) had been previously investigated by kinetic analysis [8, 9]. Therefore, the remaining hinge regions of 129–135 and 141–145, which are located between the thumb and finger regions, were selected for further study. In the two hinge regions, Val131, Arg132, Asn141, and Ala142 were chosen because these residues are located at the edges of the secondary structure, which could be the location of the core mechanical hinges [6] and are not considered to disrupt the secondary protein structures correlated with its functional activity. As shown in Fig. 2, these residues are located in the connecting region of the two atomic clusters

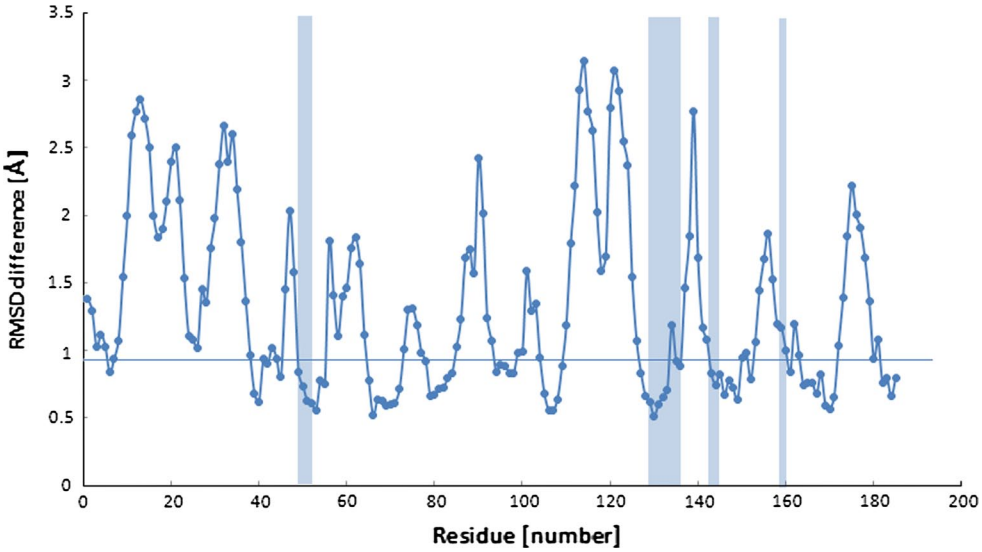

Fig. 1 Residual fluctuation calculated by FRODAN. The colored parts are the hinge regions, 49–51, 129–135 and 142–145, 159–160 from *left* to *right*

Table 3 Residual fluctuations calculated by FRODAN

Structure	Average of entire residue (Å)	Average of hinge region (Å)	Minimum (Å)	Maximum (Å)
Apo	1.32	0.893	0.517	3.14
Substrate-bound	1.46	1.27	0.584	4.51

containing catalytic residues (Glu78, Glu172), which indicates that the residues are located in the hinge region.

To investigate amino acid flexibility and the activity relationship, the target sites Val131, Arg132, Asn141 and Ala142 were mutated to several different amino acids; Val131 to Ser; Arg132 to Met and Leu; Asn141 to Gly, Thr and Val; and Ala142 to Ile. The above amino acids were selected to substitute for the wild-type residues because their residue flexibilities differ from the original residues according to their amino acid B-factor profile (Table 4), and the strength of the intra-molecular interactions of the residues could be changed by the mutation.

The mutants generated in the previous studies (R49N, R49E, R49Q, H156V) were also analyzed using in silico mutations. The alterations of the intra-protein interactions were analyzed using PIC, and the results are shown in Table 5.

Kinetic analysis of the mutants

In general, enzyme activity is represented as V_{max} (k_{cat}), while the enzyme efficiency is represented as V_{max}/K_m, which takes into account the binding affinity of the enzyme to its substrate. This study focused on the increase in catalytic activity that occurs when an enzyme is reacting with excess substrate. For the evaluation of the activities of

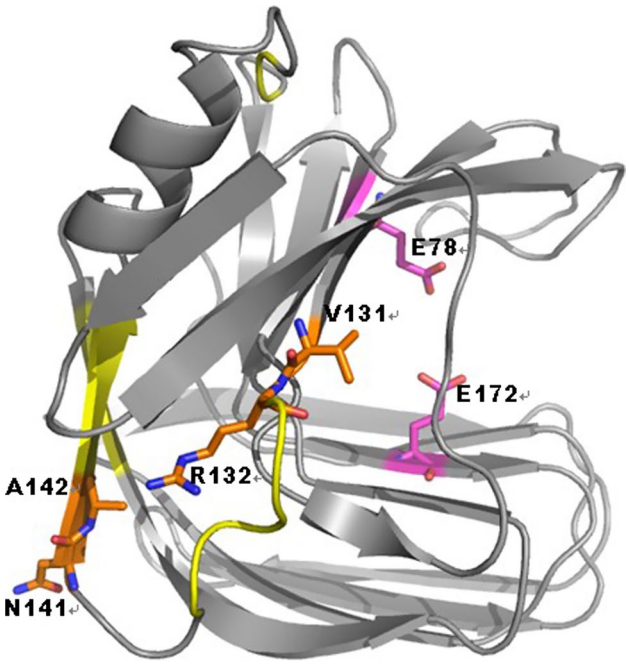

Fig. 2 Target residues of Bcx (PDB: 1XNB). The hinge regions were in *yellow*, the target residues (V131, R132, N141, A142) are in *orange* and the catalytic residues (E78, E72) are in *pink* represented by stick diagram (color figure online)

the wild-type enzyme and the seven mutants, three from the hinge region 129–135 and four from the hinge region 141–145, a kinetic analysis was carried out. The V_{max} values were calculated with the Lineweaver–Burk equation [11] using the xylose standard curves generated in each substrate concentration (Table 6). As a result, the V_{max} values of R132L, N141T, N141V and A142I improved, while those of V131S, R132L and N141G decreased or were maintained.

Table 4 Amino acid flexibility index (B-factor profile) [18]

Amino acid[a]																		
W	C	F	I	Y	V	L	H	M	A	T	R	G	Q	S	N	P	D	E	K

[a] The order of the amino acids from left to right indicates the most buried (rigid) to the most exposed (flexible)

Table 5 Intra-protein interactions of wild type and mutants calculated by PIC (analysis of the previous study)

Enzyme	Hydrophobic interaction	Intra-protein hydrogen bond			Additional interaction
		Main chain–main chain	Main chain–side chain	Side chain–side chain	
WT(49)		F146(N)–R49(O)	R49(NH1)–T44(O)	R49(NE)–Q167(OE1)	W42–R49 (cation–pi)
R49N		F146(N)–N49(O)	S46(N)–N49(ND2)	N49(ND2)–Q167(OE1) Q167(OE1)–N49(ND2)	
R49E		F146(N)–E49(O)	S46(N)–E49(OE2) E49(OE2)–T44(O)	E49(OE1)–Q167(OE1)	
R49Q		F146(N)–Q49(O)	S46(N)–Q49(NE2) Q49(NE2)–T44(O)	Q49(OE1)–Q167(OE1) Q49(NE2)–Q167(OE1)	
WT (156)		H156(N)–A152(O) H156(N)–W153(O) H156(N)–K154(O) M158(N)–H156(O)	H156(NE2)–K95(O) H156(ND2)–A152(O)		
H156V	I107–V156 W153–V156 V156–M158	V156(N)–A152(O) V156(N)–W153(O) V156(N)–K154(O) V158(N)–H156(O)			

Thermostability of the mutants

The T_m values of the mutants were compared to that of the wild-type xylanase (Fig. 3). V131S and R132M showed the same thermodynamic stability as the wild type. Other mutants also exhibited almost the same T_m values with slight decrease, 1 °C (R132L, N141G, and N141T) or 2 °C (N141V and A142I) lower. The results indicate that the stability of the variants was not significantly changed, and has no significant problems in the point of practical applications.

Analysis of the hinge region between the thumb and finger (near the thumb)

The structure of Bcx is analogous to the features of a right hand, containing an α-helix and two β-sheets forming a β-sandwich. Both β-sheets comprise a twisted backbone and form a cleft where xylose residues bind. Two conserved glutamic acids acting as catalytic residues are on opposite sides of the cleft.

The hinge region of 129–135 is located in the connecting site of the finger and the thumb of Bcx, which is known to be the most flexible region in the enzyme and important for catalysis [16]. In addition, this region is the most deformed atomic group in terms of RMSD value, which occurs when the apo and holo forms are superimposed.

Table 6 Kinetic parameter values for wild-type and mutant Bcx (this study)

Hinge region	Enzyme[a]	Rigidity[b]	V_{max} (mM/min)[c]	K_m (mM)[c]	V_{max}/K_m (1/min)[c]
–	Wild type	–	66.7	5.53	12.0
129–135	V131S	Flexible	31.3	2.78	11.2
	R132M	Rigid	75.2	5.51	13.6
	R132L	Rigid	45.7	2.49	18.3
141–145	N141G	Flexible	64.1	5.56	11.5
	N141T	Rigid	90.9	6.73	13.5
	N141V	Rigid	131	15.6	8.45
	A142I	Rigid	75.8	6.27	12.1

[a] The same concentration of enzymes (100 ng/ml) was used for kinetic analysis

[b] The flexibility of the introduced amino acid compared to the original according the amino acid B-factor profile (Table 1.) "Flexible" (or "Rigid") indicates a more flexible (or rigid) amino acid than the original was introduced

[c] Because beechwood xylan is a polymeric substrate, the substrate concentration was transformed into a product (xylose) concentration scale considering the weight concentration of the substrate and the molecular weight of xylose

Near the hinge region, three mutants were generated––V131S, R132M and R132L. In the case of Val131, the original amino acid Val is listed as a relatively rigid one

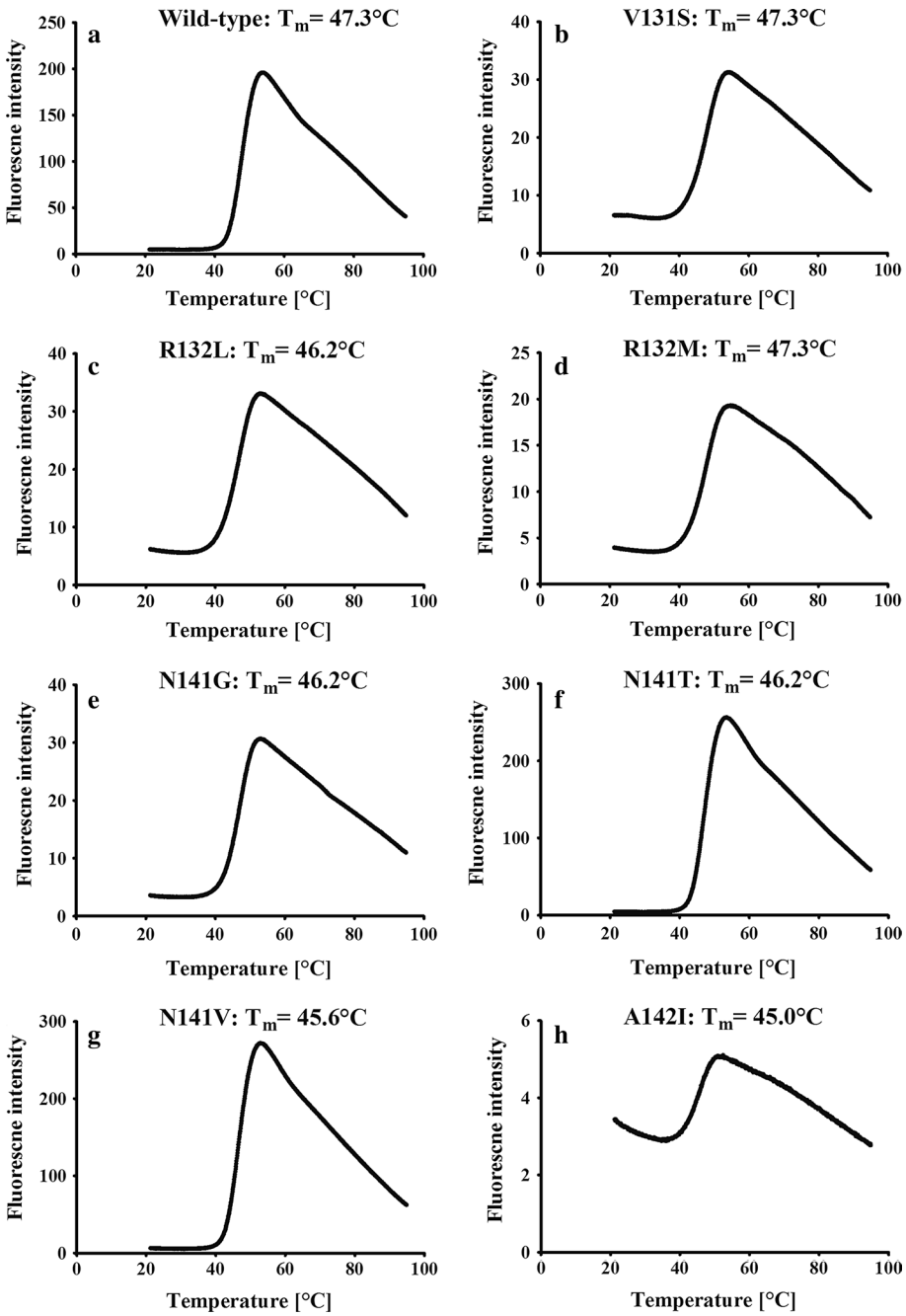

Fig. 3 Thermodynamic stability of the wild-type and mutant xylanases measured by differential scanning fluorimetry (DSF)

in the amino acid B-factor profile (Table 4) and can contribute to the rigid structure by forming hydrophobic interactions. This site was substituted with Ser, which is more flexible than Val. In addition, Val131 lost all five hydrophobic interactions (Table 7) as a result of in silico mutation, implying that the rigidity of the residue maintained by hydrophobic interactions decreased; therefore, it is estimated that flexibility was increased after the substitution. In the experimental mutation of V131S, V_{max} decreased to 47 % of wild type. This decrease may be due to increased mobility and flexibility of the thumb region; the constraints imposed by the hydrophobic interactions were broken, and the increased mobility may have hampered the closure of the active site pocket after the substrate binding, which is important for catalysis as it prevents the entry of water. In the case of Arg132, Arg is listed as relatively flexible in the flexibility index and is also known as a flexible amino acid because of its long side chain. This site was substituted with Met and Leu; both of these residues are more rigid than the original Arg and can create hydrophobic interactions. As a result of the mutations, new hydrophobic interactions were generated in both of the substitutions (Table 7), implying that the rigidity of site 132 may have been intensified. However, the cation–pi interaction was

Table 7 Intra-protein interactions of wild type and mutants calculated by PIC

Enzyme	Hydrophobic interaction	Intra-protein hydrogen bond		Additional interaction
		Main chain–main chain	Main chain–side chain	
WT(131)	V82–V131 W85–V131 P90–V131 Y108–V131 W129–V131	N106(N)–V131(O) V131(N)–N106(O) Q133(N)–V131(O)	R89(NH1)–V131(O)	
V131S		N106(N)–S131(O) S131(N)–N106(O) Q133N(N)–S131(O)	R89(NH1)–S131(O)	
WT(132)		R132(N)–V82(O) S134(N)–R132(O)	R89(NE)–R132(O) R89(NH1)–R132(O) R132(NH2)–S134(O)	Y105–R132 (cation–pi interaction)
R132M	W85–M132 Y105–M132	M132(N)–V82(O) S134(N)–M132(O)	R89(NE)–M132(O) R89(NH1)–M132(O) R136(N)–M132(SD)	Y105–M132 (aromatic–sulphur interactions)
R132L	W85–L132 Y105–L132	L132(N)–V82(O) S134(N)–L132(O)	R89(NE)–L132(O) R89(NH1)–L132(O)	

Enzyme	Hydrophobic interaction	Intra-protein hydrogen bond		Cation–pi interaction
		Main chain–main chain	Main chain–side chain	
WT(141)			N141(N)–N54(OD1)	
N141G			G141(N)–N54(OD1)	
N141T			T141(N)–N54(OD1)	
N141V	V141–W185		V141(N)–N54(OD1)	
WT(142)	Y53–A142	Y53(N)–A142(O) A142(N)–Y53(O) A142(N)-S140(O)		
A142I	Y53–I142 I142–I144	Y53(N)–I142(O) I142(N)–Y53(O) I142(N)–S140(O)		

broken in R132L, which may have weakened the rigidity. The experimental mutations of R132M and R132L showed 113 and 69 % of the wild-type V_{max}, respectively. Both substituted amino acids may have created hydrophobic interactions, but the V_{max} of R132M increased while that of R132L decreased. Possible explanations for this result may include the shape of the amino acid and the loss of the cation–pi interaction. The Met side chain is a simple line, similar to the original amino acid Arg; in contrast, the Leu side chain is branched. This branched side chain could create a broad atomic surface, which may lead to collisions with neighboring amino acids. Additionally, this substitution could disrupt the cation–pi interaction with Tyr105, which would create negative effects in the fluctuation of the thumb region and, thus, enzyme activity.

Analysis of the hinge region between the thumb and finger (near the finger)

The hinge region 141–145 is located in the bent β-strand connecting the two atomic groups that each contains catalytic glutamic acid. At the edge of the β-strand, each mutation of N141G, N141T, N141V and A142I was carried out. Among the substituted amino acids at N141, Gly is more flexible than Asn; in contrast, Thr and Val are more rigid than Asn (Table 4). From the analysis performed by the in silico mutation and protein interactions calculator (PIC), it was found that N141G and N141T generated no changes in intra-molecular interactions. However, Thr has more rigid properties, according to the B-factor index (Table 4). In the case of N141V, formation of a new hydrogen bond could occur (Table 7). Although a hydrogen bond is a relatively weak interaction, it has a critical role in protein folding, and its strength is proportional to the numbers of and inversely proportional to the distance between the atoms forming the bond [4]. Experimental results show that V_{max} of N141G is almost equal to that of wild type, whereas V_{max} of N141T and N141V increased to 136 and 196 %, respectively (Table 6). The reason for the increased V_{max} could be related to the structural rigidity of the region introduced by additional hydrogen bonds or hydrophobic interactions. In the case

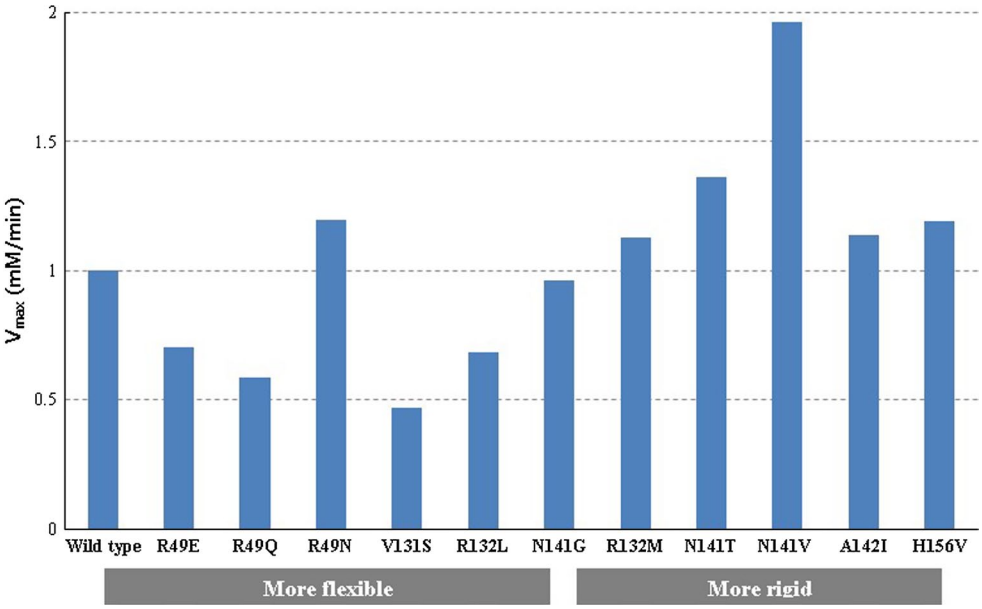

Fig. 4 Relative V_{max} values of wild type and all mutants of the previous and this study. "More flexible" (or "More rigid") represents the alteration in the flexibility of the mutated residue in terms of the intra-protein interactions

of A142, the residue was substituted with the more rigid amino acid Ile, which may have added a hydrophobic interaction, indicating that the local structural rigidity increased. In the experimental results, the mutant showed 113 % V_{max} of wild type. From these results, it can be observed that the V_{max}-enhanced mutants have a tendency to exhibit more rigid local structures.

The relationship between hinge flexibility and catalytic activity

Out of the seven mutants generated in the hinge region, the four mutants V131, R132, N141 and A142 showed increased V_{max} (Table 6). It was observed that more rigidly substituted mutants (R132M, N141T, N141V and A142I) showed increased V_{max} and that more flexibly substituted mutants (V131S and N141G) showed decreased V_{max} (Fig. 4). The results of previous mutational studies (R49E, R49Q and H156V) contribute to the confirmation of this tendency [8, 9].

In contrast to the enhancement of V_{max}, V_{max}-improved mutants worsen their substrate binding as represented by their K_m value. One reason for this may be that though substitution with a more rigid amino acid allowed the maintenance of the catalysis conformation after substrate binding, it could not induce the freedom required for substrate binding. Another reason for worsened substrate binding may be related to the role of the N141 site, a secondary substrate-binding site that leads to enhanced substrate affinity in cooperation with the active site, thus increasing the catalytic activity [12]. The reason for the worsened substrate binding of this site may be the negative modulation of the secondary binding site.

Conclusions

The relationship between hinge flexibility and activity was investigated with the model enzyme of *B. circulans* xylanase, which has hinge-bending motions during catalysis. Computational tools were applied for the identification of the hinge region. V131, R132, N141 and A143 were selected as hinge residues and mutated to alter the flexibility according to amino acid B-factor profile and the intensity of the intra-molecular interactions. Val131 and R132 are located in and near the edge of the β-strand of the most flexible thumb region of Bcx, and the mutant substituted with a more flexible amino acid showed decreased V_{max} (V131S), whereas the mutant substituted with a more rigid amino acid showed increased V_{max} (R132M). Asn141 and Ala142 in the connector between two quasi-rigid bodies containing catalytic residues were both mutated to several different amino acids (N141G, N141T, N141V and A142I). From the kinetic analysis, it was revealed that V_{max} tends to increase with the rigidity of the hinge region. In summary, the rigidified hinge region enhanced the activity (V_{max}) of the enzyme.

References

1. Bailey MJ, Biely P, Poutanen K (1992) Interlaboratory testing of methods for assay of xylanase activity. J Biotechnol 23(3):257–270
2. Bradford MM (1976) A rapid and sensitive method for the quantitation of microgram quantities of protein utilizing the principle of protein dye binding. Anal Biochem 72(1–2):248–254
3. Fisher CL, Pei GK (1997) Modification of a PCR-based site-directed mutagenesis method. Biotechniques 23(4):570–574

4. Frey PA (2001) Strong hydrogen bonding in molecules and enzymatic complexes. Magn Reson Chem 39((Spec. Iss.)):S190–S198
5. Hammes GG (2002) Multiple conformational changes in enzyme catalysis. Biochemistry 41(26):8221–8228
6. Hayward S (1999) Structural principles governing domain motions in proteins. Proteins Struct Funct Genet 36(4):425–435
7. Hayward S, Berendsen HJC (1998) Systematic analysis of domain motions in proteins from conformational change: new results on citrate synthase and T4 lysozyme. Proteins Struct Funct Genet 30(2):144–154
8. Joo JC, Pack SP, Kim YH, Yoo YJ (2011) Thermostabilization of *Bacillus circulans* xylanase: computational optimization of unstable residues based on thermal fluctuation analysis. J Biotechnol 151(1):56–65
9. Kim T, Joo JC, Yoo YJ (2012) Hydrophobic interaction network analysis for thermostabilization of a mesophilic xylanase. J Biotechnol 161(1):49–59
10. Krivov GG, Shapovalov MV, Dunbrack RL Jr (2009) Improved prediction of protein side-chain conformations with SCWRL4. Proteins Struct Funct Bioinform 77(4):778–795
11. Lineweaver H, Burk D (1934) The determination of enzyme dissociation constants. J Am Chem Soc 56(3):658–666
12. Ludwiczek ML, Heller M, Kantner T, McIntosh LP (2007) A Secondary xylan-binding site enhances the catalytic activity of a single-domain family 11 glycoside hydrolase. J Mol Biol 373(2):337–354
13. Ma B, Shatsky M, Wolfson HJ, Nussinov R (2002) Multiple diverse ligands binding at a single protein site: a matter of preexisting populations. Protein Sci 11(2):184–197
14. Muilu J, Törrönen A, Peräkylä M, Rouvinen J (1998) Functional conformational changes of endo-1,4-xylanase II from Trichoderma reesei: a molecular dynamics study. Proteins Struct Funct Genet 31(4):434–444
15. Plesniak LA, Wakarchuk WW, McIntosh LP (1996) Secondary structure and NMR assignments of *Bacillus circulans* xylanase. Protein Sci 5(6):1118–1135
16. Pollet A, Vandermarliere E, Lammertyn J, Strelkov SV, Delcour JA, Courtin CM (2009) Crystallographic and activity-based evidence for thumb flexibility and its relevance in glycoside hydrolase family 11 xylanases. Proteins Struct Funct Bioinform 77(2):395–403
17. Potestio R, Pontiggia F, Micheletti C (2009) Coarse-grained description of protein internal dynamics: an optimal strategy for decomposing proteins in rigid subunits. Biophys J 96(12):4993–5002
18. Radivojac P, Obradovic Z, Smith DK, Zhu G, Vucetic S, Brown CJ, Lawson JD, Dunker AK (2004) Protein flexibility and intrinsic disorder. Protein Sci 13(1):71–80
19. Schein CH, Noteborn MHM (1988) Formation of soluble recombinant proteins in *Escherichia coli* is favored by lower growth temperature. BioTechnology 6(3):291–294
20. Schramm AM, Mehra-Chaudhary R, Furdui CM, Beamer LJ (2008) Backbone flexibility, conformational change, and catalysis in a phosphohexomutase from *Pseudomonas aeruginosa*. Biochemistry 47(35):9154–9162
21. Schulz GE (1991) Domain motions in proteins. Curr Opin Struct Biol 1(6):883–888
22. Sime JT (1999) Applications of biocatalysis to industrial processes. J Chem Educ 76(12):1658–1661
23. Subramaniyan S, Prema P (2002) Biotechnology of microbial xylanases: enzymology, molecular biology, and application. Crit Rev Biotechnol 22(1):33–64
24. Sung WL, Luk CK, Zahab DM, Wakarchuk W (1993) Overexpression of the *Bacillus subtilis* and *circulans* xylanases in *Escherichia coli*. Protein Expr Purif 4(3):200–206
25. Tina KG, Bhadra R, Srinivasan N (2007) PIC: protein interactions calculator. Nucleic Acids Res 35(Suppl.2):W473–W476
26. Wells S, Menor S, Hespenheide B, Thorpe MF (2005) Constrained geometric simulation of diffusive motion in proteins. Phys Biol 2(4):S127–S136
27. Yon JM, Perahia D, Ghélis C (1998) Conformational dynamics and enzyme activity. Biochimie 80(1):33–42
28. Zheng L, Baumann U, Reymond JL (2004) An efficient one-step site-directed and site-saturation mutagenesis protocol. Nucleic Acids Res 32(14):e115